



LAWRENCE  
LIVERMORE  
NATIONAL  
LABORATORY

# High Order Ribbon Fiber Modes, Simulations, and Experiments for High Power Amplifiers

D. Drachenberg, M. Messerly , P. Pax, A.  
Sridharan, J. Tassano, J. Dawson

February 13, 2013

Photonics West 2013  
San Francisco , CA, United States  
February 4, 2013 through February 7, 2013

## **Disclaimer**

---

This document was prepared as an account of work sponsored by an agency of the United States government. Neither the United States government nor Lawrence Livermore National Security, LLC, nor any of their employees makes any warranty, expressed or implied, or assumes any legal liability or responsibility for the accuracy, completeness, or usefulness of any information, apparatus, product, or process disclosed, or represents that its use would not infringe privately owned rights. Reference herein to any specific commercial product, process, or service by trade name, trademark, manufacturer, or otherwise does not necessarily constitute or imply its endorsement, recommendation, or favoring by the United States government or Lawrence Livermore National Security, LLC. The views and opinions of authors expressed herein do not necessarily state or reflect those of the United States government or Lawrence Livermore National Security, LLC, and shall not be used for advertising or product endorsement purposes.

# High Order Ribbon Fiber Modes, Simulations, and Experiments for High Power Fiber Amplifiers

Derrek Drachenberg\*, Michael Messerly, Paul Pax, Arun Sridharan, John Tassano, Jay Dawson

Lawrence Livermore National Lab, L-491, P.O. Box 808, Livermore, CA 94551, USA

[\\*drachenberg1@llnl.gov](mailto:*drachenberg1@llnl.gov)

## ABSTRACT

Diffraction limited fiber amplifiers in a circular geometry are likely to be limited by nonlinearities to 2 kW for narrowband and 10-36 kW for broadband lasers. We have proposed a ribbon fiber geometry to allow scaling fiber lasers above these limits in which a high order ribbon mode is amplified and converted back to the fundamental mode in free space. Novel methods of illuminating a high order ribbon fiber mode are discussed and compared with modeling and experimental results showing high purity illumination, > 90%. A 10 kW single frequency ribbon fiber amplifier design is presented and BPM simulation results verify the approach.

## 1. INTRODUCTION

Extremely high power diffraction-limited lasers are needed for projected research, defense, and manufacturing applications. The power generated from conventional fiber lasers – those based on fibers having cores with circular cross-sections - has risen significantly over the last decade<sup>1</sup>. Today 10 kW fiber lasers are commercially available, but these may be approaching fundamental limits; tradeoffs between thermal lensing [inversely proportional to area] and either stimulated Brillouin scattering (SBS) or stimulated Raman scattering (SRS) [proportional to area] are expected to limit the power to 2 kW for narrowband, SBS-limited sources or 36 kW for broadband, SRS-limited sources. In addition to these limits, bending induced mode distortion limits large circular-core fibers to mode field diameters of roughly 50  $\mu\text{m}$ , and at that size, SRS will likely limit broadband fiber laser amplifiers to powers of roughly 10 kW<sup>2</sup>.

Beam combining techniques sidestep the limits of individual fiber lasers and amplifiers by combining many lasers into a single, brighter beam<sup>3–8</sup>. Higher power unit cells benefit all such approaches by reducing the number of cells required to reach a target combined output power.

We present here a novel method for scaling the power of single emitters beyond their current limits. The method involves transitioning away from traditional circular-core fiber amplifiers to rectangular-core fiber amplifiers. A rectangular (hereafter, ribbon) core has a larger surface area than a circular core for the same enclosed core volume, and thus radiates heat more efficiently. The geometry also raises the nonlinear thermal lensing limit because the thermal gradient in the wide dimension has a nearly flat top profile, leaving the thermal lensing to be limited by the width and numerical aperture of the single mode narrow dimension. A ribbon core also sidesteps bending limits, provided the fiber is selectively bent about its narrow axis. A ribbon core thus can be made large enough to significantly raise its SBS and SRS limits without making it thermal-lensing or bending limited.

Larger cores generally allow additional propagation modes. Though these can be problematic, they have an important advantage: compared to the fundamental, high order modes are more stable (there is a larger separation between their propagation constants and those of their neighboring modes<sup>9</sup>). Unlike the high order modes of a circular core, all lobes of all modes of a ribbon core have the same peak intensity. Thus, ribbon-core fibers can propagate and amplify power in a high-order mode without suffering from hotspot-precipitated nonlinearities or damage. The high order modes of a ribbon-core fiber are consequently preferred, provided they can be cleanly excited from the TEM<sub>00</sub> mode of a seed laser, amplified without distortion, and efficiently converted back to a TEM<sub>00</sub> beam – spatially analogous to chirped pulse amplification, where a pulse is stretched in time, amplified, and then recompressed.

Others have investigated ribbon core fibers but have either taken a multi-core approach<sup>10</sup> (in that reference, incoherent cores) or have focused on fibers that propagate the fundamental mode but with weakly-guided high order modes<sup>11–13</sup>. An active ribbon fiber operating in a high order mode has been previously demonstrated<sup>14</sup>, but refractive index non-uniformity across the core created modal impurities, and its relatively more absorptive, low melting-temperature phosphate-based glass limited its power to less than 1 W. Selective mode excitation in ribbon-core fibers<sup>15</sup> and efficient conversion from a high-order ribbon mode to a TEM<sub>00</sub> beam<sup>16</sup> has already been demonstrated by the use of programmable phase plates.

In this paper, we first discuss a design methodology for SBS limited ribbon fiber amplifiers which leads to a design for a single frequency 10 kW ribbon fiber amplifier (§ 2). Then we report simulation results via the beam propagation method (BPM) which validate the design and ribbon fiber approach to mitigating nonlinear thermal lensing (§ 3). Next we report a novel technique for excitation of a single high order mode in a ribbon fiber (§ 4.1-4.2) and demonstrate this technique in an LLNL fabricated, un-doped, double-clad, PCF ribbon fiber (§ 4.3). The mode excitation technique reported here differs from past work in that it uses a binary phase plate, a more flexible approach that achieves higher modal purity. The ribbon fiber presented here also differs from past work in that it is all silica rather than phosphate glass, and the core is guided by air holes that lower the average index in the region surrounding the core.

## 2. SBS LIMITED AMPLIFIER DESIGN METHODOLOGY AND SOLUTION FOR 10 KW

The design of an SBS limited (narrowband) fiber laser amplifier is similar for both a ribbon and a circular cross-section fiber. The reason that the ribbon fiber can likely be scaled to higher powers than the circular cross-section fiber is that the core area can be scaled up to increase the SBS limited threshold power, while the thermal lensing limit is not approached by the increase in area, as would be the case for a circular cross-section fiber. In this case, thermal lensing can be ignored in the design process, and is checked by simulation.

The threshold for the onset of SBS for a narrow band fiber laser is given by equation (1) below<sup>2</sup>,

$$P_{out}^{SBS} \approx \frac{17 \cdot A_{eff}}{g_B(\Delta\nu) \cdot L_{eff}} \quad (1)$$

$$L_{eff} = \frac{1}{g} (e^{g \cdot L} - 1) \quad (2)$$

$$A_{eff} = \Gamma^2 \cdot \pi \cdot a^2 \quad (3)$$

$$g = \frac{\text{Log}(G)}{L} \quad (4)$$

where  $g_B(\Delta\nu)$  is the Brillouin gain, assumed to be  $5 \times 10^{-11}$ <sup>17</sup>,  $a$ , the effective radius of fiber core area,  $A_{eff}$ , the effective area considering modal overlap,  $L_{eff}$ , the effective fiber length given a particular gain coefficient,  $g$ , and  $\Gamma$ , is the electric field modal overlap with fiber core area. Some specialty fiber designs aim to mitigate SBS, and to whatever factor this is accomplished, the results and conclusions in this paper could be appropriately reevaluated.

However, in this paper no such SBS mitigation designs are considered. Combining equations (1) through (4) gives the format of equation (5) below which is used in the following amplifier design process.

$$P_{out}^{SBS} \approx \frac{17 \cdot A_{eff}}{g_B(\Delta\nu) \cdot L} \ln(G) \quad (5)$$

The above equation gives the maximum power from the output of an amplifier that can be generated given the core mode area,  $A_{eff}$ , modal overlap,  $\Gamma$ , fiber length,  $L$ , and total amplifier gain,  $G$  before becoming SBS limited. For any desired output power, it is straightforward to plot the necessary fiber length vs. mode area to stay below the SBS limit, and this plot illustrates a broad range of solutions. However, it is valuable to find the solution which provides the smallest possible core area, to reduce the number of guiding modes.

The SBS limited power threshold is proportional to mode area,  $A_{eff}$ , and inversely proportional to fiber length. It is tempting to reduce the fiber length, and core area in balanced proportion until the fiber is as small as desired. However, for a particular fiber design, with mode area,  $A_{eff}$ , cladding area,  $A_{CL}$ , and core absorption  $\alpha$ , there is a particular length of fiber that will be required to absorb all the pump power for a given brightness of pump. Here, we show that the shortest length, and subsequently the smallest fiber core, for an SBS limited amplifier is determined by the pump brightness and can be approximated by a single equation.

Equation (3) will give an approximate length for a fiber to absorb the pump power to the 20 dB level. Commercially available ytterbium doped glasses can be purchased which will absorb 250 dB/m at 976 nm, a typical pump wavelength for ytterbium lasers.

$$L \approx \frac{A}{\alpha_p} \cdot \frac{A_c}{A_{eff}} \Gamma^2 \quad (6)$$

Equation (7) gives the brightness of the pump cladding,

$$B = \frac{P_p}{\pi(w_{CL})^2 \cdot \pi(\theta_{CL})^2} \approx \frac{P_p}{A_{CL} \cdot \pi(NA_{CL})^2} \quad (7)$$

where  $P_p$  is the pump power,  $w_{CL}$  is the cladding radius, and  $NA_{CL}$  is the cladding numerical aperture.

The required area of the cladding,  $A_{CL}$ , can be determined solely by equation (7) for a given pump power, brightness, and numerical aperture. Combining equations (4), (5), and (6), results in equation (8) for the minimum length that a fiber amplifier must be to remain in the SBS limited regime. Amplifiers with shorter lengths will be limited by available pump brightness. Amplifiers with longer lengths will need to have larger cores to stay under the SBS limit described by equation (5).

$$L_{min} \approx \sqrt{\frac{17 \cdot \Gamma^2 \cdot \ln(G) \cdot A}{g_B(\Delta\nu) \cdot \eta_{laser} \cdot B_{pump} \cdot \pi \cdot NA_{CL}^2 \cdot \alpha_{core}}} \quad (8)$$

Using only equations (5) for the SBS limited output power, and equation (8) for the optimal length, an estimated design can be calculated. Keep in mind however, that for a heavily saturated amplifier, a full rate-equation model is required to provide an accurate solution. For this design, we have chosen  $B = 1.2 \times 10^{11} \text{ W} / \text{sr} \cdot \text{m}^2$  as the commercially

available diode pump brightness, a cladding NA of 0.45, amplifier efficiency of  $\eta = 0.9$ , and desired amplified output power of 10 kW. From (7), one can calculate the cladding area to be  $A_{CL} = 1.43 \times 10^5 \mu m^2$ . If a linear gain of  $G = 100$  is chosen, according to Equation (8), the necessary fiber length must be  $L = 1.1$  m. Having length and output power, one can use equation (5) to calculate the necessary mode area,  $A_{eff} = 7.0 \times 10^3 \mu m^2$ .

This estimated design was checked against a 3-level fiber amplifier model following the Giles methodology<sup>18</sup>. The results of solving the partial differential equations of the 3-level amplifier model show that the pump is not completely absorbed based on the estimated length from equation (8) with 10% of the pump power exiting at the output. Therefore, the fiber should be lengthened to increase absorption, and the core size increased to stay under the SBS threshold determined by equation (5). By iteratively increasing the fiber length and core size along the curve generated by equation (5), the length of 1.7 m, and the mode area of  $A_{eff} = 10.9 \times 10^3 \mu m^2$  is found to result in the desired amplifier specifications of 10 kW output, with 20 dB pump absorption, and 89% efficiency. The increased core mode area suggests a ribbon fiber with a  $500 \times 34 \mu m$  core, or an effective core diameter of  $D_{eff} = 146 \mu m$ . The effective core diameter is defined by equation (9), and represents the core diameter a fiber with a mode area,  $A_{eff}$ , and mode/core area overlap ratio,  $\Gamma^2$ , if its core were circular.

$$D_{eff} = \frac{2}{\Gamma} \sqrt{\frac{A_{eff}}{\pi}} \quad (9)$$

Fig. 1 shows the SBS limited length vs. core diameter curves for 4 different desired output power levels. For lengths above the horizontal line an amplifier is SBS limited, while for lengths below the line an amplifier is limited by available pump power and cannot reach the SBS limited power. The optimal fiber design with the smallest possible core areas for a particular output power level lies at the intersection of the SBS limited curve and the horizontal line representing a balance between the SBS limited region and the pump power limited region.

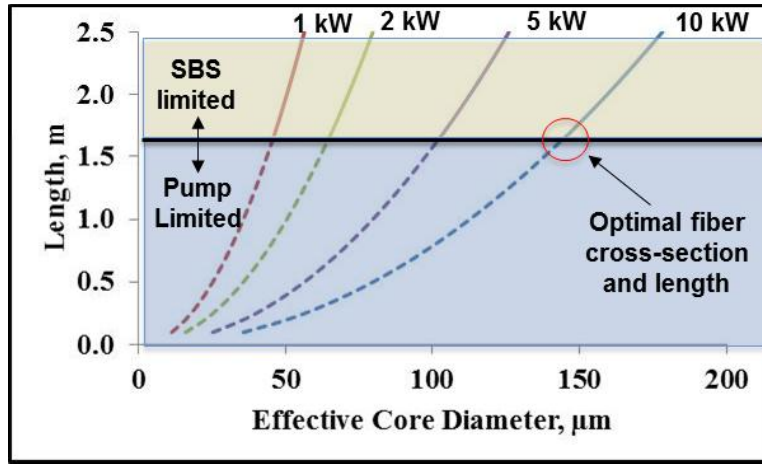


Fig. 1: SBS limited length and effective core diameters for four different power levels. For lengths above the horizontal line an amplifier is SBS limited, while for lengths below the line an amplifier is limited by available pump power and cannot reach the SBS limited power.

The intensity of  $0.9 \text{ W/cm}^2$  is well under the optical damage threshold of  $10 \text{ W/cm}^2$  for silica<sup>19</sup>. So far, the entire design process is not dependent on the rectangular structure, and all calculations and results are also true for diffraction limited circular core fibers. A circular core fiber, however, would be additionally limited by thermal lensing

to < 2 kW. A ribbon fiber of this core area is still SBS limited, not thermal lens limited, due to the flat top nature of its thermal cross-section.

A ribbon core fiber can be made with a 500  $\mu\text{m}$  width and a 34  $\mu\text{m}$  height to satisfy the area requirements of the above design for a 10 kW narrowband fiber amplifier. This fiber could be operated in a single high order mode in the wide dimension which would then be converted back to the  $\text{TEM}_{00}$  mode in free space. We have previously demonstrated the capability to convert a ribbon mode to the  $\text{TEM}_{00}$  mode<sup>16</sup>. The width of 500  $\mu\text{m}$  was chosen arbitrarily as the size of fiber which can no doubt be manufactured. Greater widths are clearly possible, but will not be considered in this paper.

The narrow dimension for this result, 34  $\mu\text{m}$ , is too big to be truly single mode, but could operate in a “quasi” single mode regime; where for a particular bend radius the two higher order modes are lossy. Alternatively, at these short lengths, it is reasonable to keep a fiber straight to maintain single mode status. More details about the modal structure of this ribbon fiber design will be discussed in a later section.

### 3. BPM SIMULATIONS FOR A 10 KW, SBS LIMITED, SINGLE HIGH ORDER MODE RIBBON FIBER AMPLIFIER

#### 3.1. Beam propagation method

A model of the ribbon fiber amplifier was developed to simulate performance. Because beam quality was a primary concern, the model was based on diffractive evolution of the signal field, which was treated, in the scalar approximation, by the well-known and robust Beam Propagation Method (BPM) [Feit & Fleck, Applied Optics, v19, 1980]. The pump light fills a much larger volume than the signal in the core, and has a much higher NA. It's treated as an intensity, evolving according to the absorption in the doped core and replenishment from the pump cladding. Amplification is treated by a simple saturable gain; because both the pump and inversion are spatially resolved, hole burning by the nonuniform signal intensity is accounted for. Finally, Kerr and thermal index non-linearities are also included. For the latter, the thermal profile is found by solving the Poisson equation, driven by local heat deposition from the absorption of pump light.

The evolution of the signal field  $E_s$  is then given by

$$\begin{aligned}
 i \frac{\partial}{\partial z} E_s(x, y) &= \frac{1}{2n_0 k_0} \left[ \nabla_{\perp}^2 + k_0^2 (n^2(x, y) - n_0^2) \right] E_s(x, y) && \text{Confinement by the waveguide} \\
 &+ i \frac{n_T \sigma_e}{2} N(x, y) E_s(x, y) && \text{Saturable gain} \\
 &+ k_0 n_2 |E_s(x, y)|^2 E_s(x, y) && \text{Kerr index variation} \\
 &+ k_0 \frac{dn}{dT} T(x, y) E_s(x, y) && \text{Thermal index variation}
 \end{aligned}$$

where the cladding and core indices are  $n_0$  and  $n(x, y)$ ;  $n_T$ ,  $N(x, y)$  and  $\sigma_e$  are the dopant density, relative inversion, and stimulated cross-section; and  $n_2$  and  $T(x, y)$  and the Kerr non-linear index and thermal profile. The signal and pump intensities *in the doped core region* are related through the inversion of the amplifying medium:

$$\begin{aligned}
 \frac{d}{dz} I_s &= (n_T \sigma_e) N I_s \\
 \frac{d}{dz} I_p &= -(n_T \sigma_a) (1 - N) I_p + (P_{p, \text{tot}} / A_{\text{tot}} - I_p) / l_{\text{mix}}
 \end{aligned}
 \quad
 N = \frac{I_p / I_{p, \text{sat}}}{1 + I_p / I_{p, \text{sat}} + I_s / I_{s, \text{sat}}}$$

The core pump intensity is depleted by absorption and replenished from the reservoir of the cladding, on a length scale  $l_{\text{mix}}$ , which depends on the area ratio of the core and cladding, and on the pump NA.

The thermal profile is found by solving the Poisson equation, with spatially resolved heat deposition and fixed temperature boundary conditions, taken to be rectangular for the sake of implementing a series solution.

$$\nabla_{\perp}^2 T(x, y) = -\frac{1}{\kappa_c} Q(x, y), \quad \text{and} \quad Q(x, y) = (n_T \sigma_a)(1 - N(x, y)) \left( \frac{\omega_p}{\omega_s} - 1 \right) I_p(x, y)$$

The BPM evolution applies the various terms in the equation above by expressing them in the space in which they are local, alternating between the spaces via FFTs. Specifically, the phase evolution due to the waveguide and the Kerr & thermal index, as well as the amplitude evolution due to the gain, are applied in real space; and the transverse Laplacian is applied in Fourier space, where it is a local operation. The thermal behavior is solved on the fiber cross-section under the approximation that we can ignore heat flow in the propagation direction. The solution is done in the Fourier domain, where again the Laplacian is local, and where Dirichlet boundary conditions are expressed as a sub-selection of allowed spatial harmonics.

### 3.2. Modes of the ribbon fiber amplifier

The modes of a ribbon fiber are similar to those of a slab waveguide, and are solved for in the same way<sup>14, 20, 21</sup>. A mode solver was used to calculate the supported modes in the 500 x 34  $\mu\text{m}$  ribbon fiber design with an NA of 0.05. The fiber supports 45 modes in the wide dimension, so the middle 22-lobed mode is chosen to be the amplifier seed as it is better confined than the highest order modes, and it has greater mode to mode isolation than the lowest order modes. As previously stated, the 34  $\mu\text{m}$  narrow dimension is too large to be truly single mode, even for an NA of 0.05, and in fact supports two and three lobed modes in the vertical dimension. However, this does not affect the result of this simulation as the fiber is assumed to be straight, and, with a length of 1.7 m, this is a reasonable assumption. It will be shown in this simulation that, even with initial modal impurities in the amplifier, the seeded mode maintains its initial purity. Furthermore, high order modes in the vertical dimension can be eliminated by winding the fiber in that dimension until all the modes which have multiple lobes in the vertical dimension are too lossy to be amplified.

Fig. 2 shows the near field amplitude and phase of the 22-lobed mode with 10% modal impurities which are randomly distributed between all the horizontal modes.

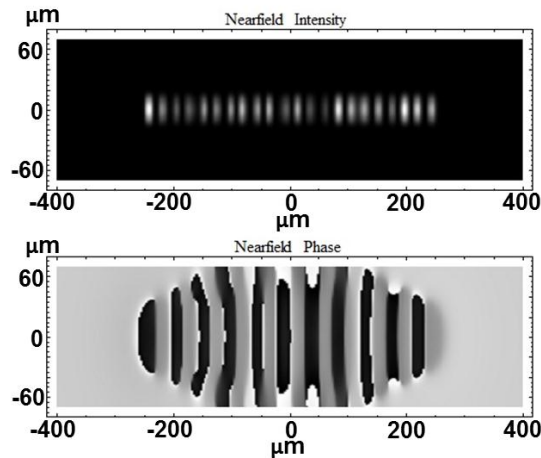


Fig. 2: Calculated near field intensity (top), phase (bottom), of the 22 lobed mode, with 10 % modal noise, used as an input seed for simulation of the 10 kW ribbon fiber amplifier



### 3.3. Simulation results

Fig. 3 shows the near field intensity and phase of the signal amplified to 10 kW. The purity of the primary 22 lobed mode is maintained at > 90 % showing that a single high order mode can be seeded into an amplifier and its purity can be maintained through amplification.

The thermal model for this simulation assumes that the edges are kept at a fixed temperature. The peak temperature rise in the longitudinal direction is less than 70 degrees, shown in Fig. 5, and the cross-sectional temperature profile at the peak temperature rise is shown in Fig. 4. These thermal gradients are well within reasonable parameters for a high power fiber laser, and the flat top nature of the cross-sectional profile demonstrates the thermal advantage the ribbon has over a circular core fiber. The simulation also confirms the mitigation of thermal lensing which was assumed in the design process.

The final output power in the signal mode is 10 kW, with 89.6 % pump to signal conversion efficiency, and a pump depletion of > 20 dB, and signal gain of 100.

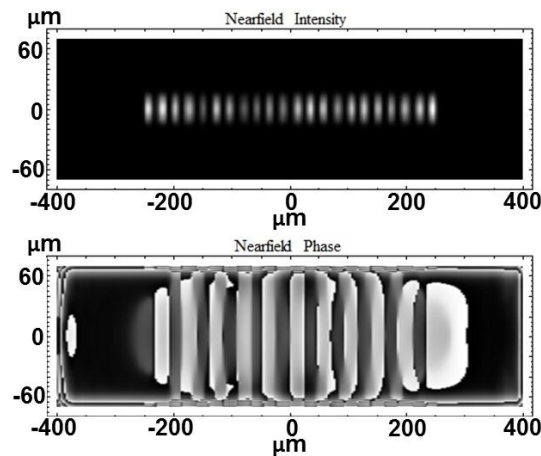


Fig. 3: Simulated 10 kW amplifier output near field intensity (top), phase (bottom), of the 22 lobed mode

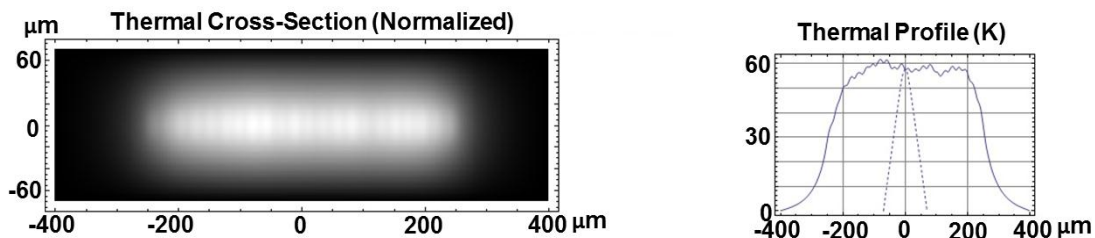


Fig. 4: Simulated thermal cross-section of ribbon fiber amplifier at location of peak temperature rise,  $z = 0.8$  m

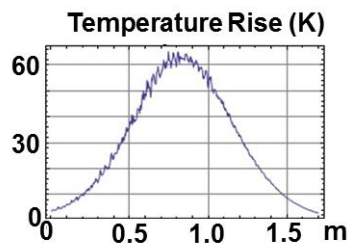


Fig. 5: Simulated temperature rise along the length of the amplifier.

## 4. ILLUMINATION OF HIGH ORDER RIBBON FIBER MODES

### 4.1. Method

Large mode-area ribbon core fibers will likely support modes with many lobes in the wide dimension. Fig. 6 illustrates the calculated near-field intensity pattern of a four lobed mode of a hypothetical ribbon fiber (NA = 0.05, core  $10 \times 100 \mu\text{m}$ ). Fig. 2 illustrates the far field of this mode; the near field peaks alternate in phase between 0 and  $\pi$ . The far field has two primary lobes, holding roughly 90% of the power, and a series of less-intense lobes between them; the number of less-intense lobes depends on the mode's order.

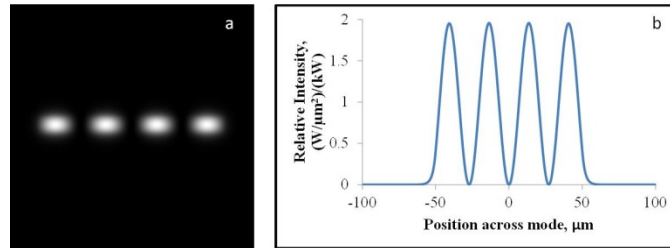


Fig. 6. Calculated near field intensity plot for a four lobed ribbon fiber mode, (a) 2D linear intensity plot, and (b) 1D linear intensity plot.

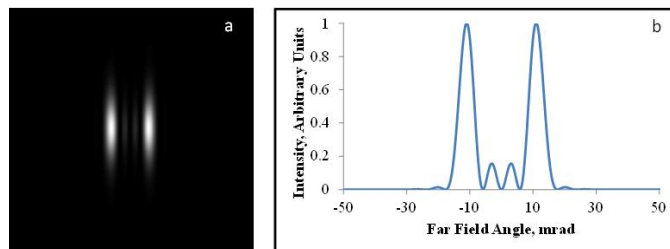


Fig. 7. Calculated far field intensity plot for a four lobed ribbon fiber mode, (a) 2D linear plot, and (b) 1D logarithmic intensity plot, 6 decades.

We have previously shown that a pair of spatial light modulators – in essence, programmable phase plates – can convert a  $\text{TEM}_{00}$  beam to a multi-lobed ribbon mode with high efficiency<sup>16</sup>. Spatial light modulators are typically only suitable for use with a few milliwatts of power. Custom, static, phase plates can also convert the beam and are suitable for high power applications<sup>22, 23</sup>, but inconvenient at this stage of our research. A third alternative, which we use here, is to convert the  $\text{TEM}_{00}$  beam to a single high-order-mode with a simple, and relatively inexpensive, binary phase plate and a cylindrical lens. In this approach, the conversion efficiency is not as high as it can be with SLMs or custom phase plates, but the purity of the illuminated mode can still reach 99%.

Laser beam quality is typically quantified by the  $M^2$  parameter or power in the bucket; however, both metrics compare the beam under test to an ideal  $\text{TEM}_{00}$  beam and are inappropriate for high order modes. Here, we compare the amplitude and phase of the field of the excited mode to those of the target mode, and define the purity as the overlap integral of the two fields. In a finished laser system,  $M^2$  can be used if the high order mode is converted back to a  $\text{TEM}_{00}$  mode<sup>16</sup>, though we do not take that step here.

### 4.2. Experimental setup and alignment procedure

Figure 3 shows the experimental setup for illuminating a high order ribbon fiber mode using a simple binary phase plate. First, a cylindrical lens focuses a collimated  $\text{TEM}_{00}$  beam in the axis perpendicular to the optical table (it remains collimated in the axis parallel to the table) and a binary phase is placed at the focal plane of the cylindrical lens. The phase plate used in this work has a half period of  $250 \mu\text{m}$ , and is 25 mm in width which gives it 100 half periods; in general, the plate should have at least as many half periods as lobes in the desired ribbon mode. The period of the

phase plate can be chosen arbitrarily since the image of the light exiting the plate will be de-magnified to match the size of the mode on the fiber end face.

The lobes of an ideal high-order ribbon-mode are of equal peak intensity. In order to illuminate a mode properly, it is necessary to illuminate the correct number of periods on the phase plate with a nearly flat top beam. A simple way to accomplish this is to overfill the phase plate illumination (in this case by a factor of three) and clip off the power outside the central region with a one dimensional spatial filter; this yields a reasonably flat illumination, though at the expense of efficiency.

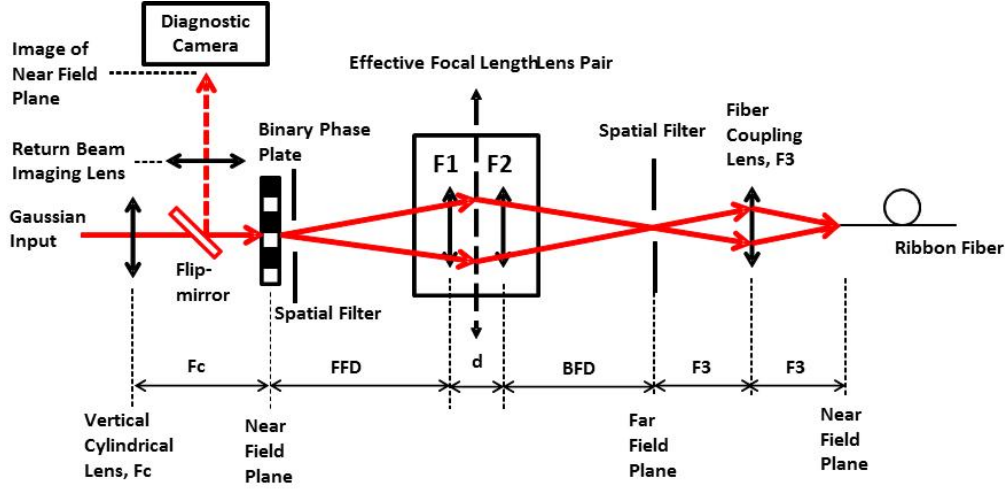


Fig. 8. Single high order ribbon fiber mode illumination experimental setup. FFD = front focal distance,  $d$  = distance between effective focal length lens pair, BFD = back focal distance.

The mode exiting the phase plate-spatial filter portion of the setup is a nearly flat top beam with a series of 0 to  $\pi$  phase shifts across it. The far field intensity pattern of this beam has two bright primary lobes (which will be matched to corresponding lobes in the far field pattern of the target mode) and a series of additional lobes at progressively higher angles of diminishing intensity. Since the latter cannot be launched into the target mode, we clip them with a spatial filter in the far field plane (as shown).

Before coupling into the fiber, the near field of the input beam must be de-magnified to match the target mode. In our setup (Fig. 8), the fiber coupling lens is an aspheric lens having a focal length of 15 mm. The effective focal length lens pair, however, can be adjusted to achieve the correct magnification. Equation (10) gives the effective focal length of the lens pair, measured from the lens pair's principal planes. Equations (11) and (12) give the front and back focal distances (measured from the principal planes); they assume the lenses in the pair are thin compared to their respective focal lengths,

$$f = EFL = \left( \frac{1}{f_1} + \frac{1}{f_2} - \frac{d}{n \cdot f_1 \cdot f_2} \right)^{-1} \quad (10)$$

$$FFD = -f + \frac{f}{f_2} \cdot d \quad (11)$$

$$BFD = f - \frac{f}{f_1} \cdot d \quad (12)$$

where  $n$  is the refractive index of the medium between the lens pair, in this case air,  $d$  is the distance between the two lenses, and  $f_1$  and  $f_2$  are the focal lengths of lenses 1 and 2, respectively.

To form an initial guess for the correct demagnification factor, we assume that the lobes of the target mode match the de-magnified phase plate, or  $N$  half-periods fit the fiber core width. An initial solution can be arrived at by dividing the product of the half period of the phase plate and the number of lobes in the desired mode by the ribbon core width. Once the demagnification factor is determined, an effective focal length for the lens pair can be calculated by multiplying the fiber coupling lens focal length by the demagnification factor. Then, an appropriate lens pair and spacing is chosen to create the desired effective focal length, and therefore to achieve the desired demagnification.

These steps yield an approximate spacing between the lenses. The spacing can be checked experimentally by reverse-propagating a beam through the fiber. The reverse beam projects an image of the core onto the phase plate, which is then imaged onto a camera. The spacing between the lens pair, and the consequent changes in front and back focal distances, can then be fine-tuned until the transitions in the phase plate fall at the appropriate positions of the core (as determined by modeling); see Fig. 9 (b).

With the demagnification properly set and forward propagation resumed, the vertical tip angle can be aligned easily by maximizing the coupled power in the forward direction. Aligning the horizontal tilt angle is not as simple and requires an additional step, one that calls for diagnostic images of the near and far field of the output in order to determine the launched modal content. In this step, the tilt of the fiber is adjusted until only two peaks are visible in the far field of the fiber output, and the desired number of lobes is visible in the near field. If the horizontal translation is inadvertently displaced during horizontal tilt alignment, the reverse propagating diagnostic can be used to realign it.

#### 4.3. High order mode excitation in a passive photonic crystal ribbon fiber

Here we report a passive photonic crystal ribbon fiber and excitation of a single higher order mode with 90% purity and a mode area of  $650 \mu\text{m}^2$ . Fig. 9 (a) shows an image of the end face of an air guided, passive, ribbon fiber. In this fiber, guiding is achieved by a set of air holes that lower the average index of the region around the core; we estimate that the fiber supports 14 modes. In a high power ribbon fiber, the outer cladding might also be rectangular to allow selective bending and better thermal control, though the fibers described in this paper all have round outer claddings.

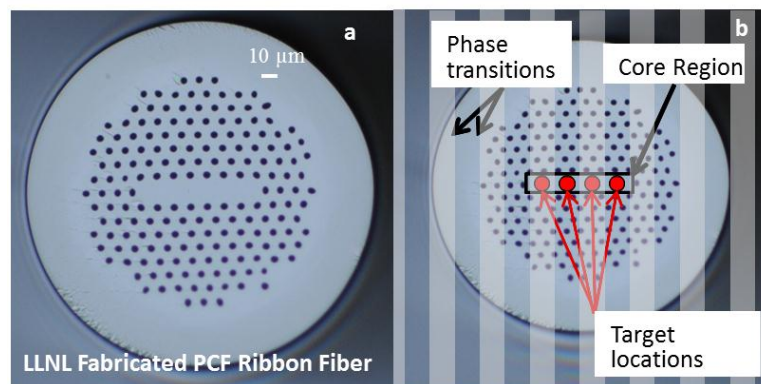


Fig. 9. (a) Photonic crystal ribbon fiber with a rectangular core cross-section, (b) An image of a ribbon fiber end face with overlaid illustrated binary phase plate transitions and target mode profile..

Using the method described in the above section, a high order five-lobed mode was illuminated with 90% purity. The purity is defined as the overlap integral of the excitation field (determined from the measured intensity distribution and the inferred phase, found via the Gerchberg-Saxton algorithm) and the expected field of the target mode<sup>24</sup>. Fig. 10 (a) and (b) show, respectively, the near- and far-field intensity distributions of expected and measured five-lobed mode

of the fiber of Fig. 9. We chose to excite a middle mode because those modes have better modal isolation than the lowest-order modes (as discussed in the introduction) and are less lossy than the highest order modes. In this case, a middle order mode is a good balance between modal isolation and high confinement.

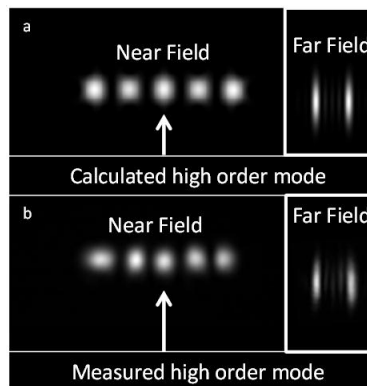


Fig. 10. The near- and far-field intensity profiles of a single five lobed mode of the photonic crystal ribbon fiber of Fig. 9, calculated (a), and measured (b).

## 5. SUMMARY

Ribbon fiber laser amplifiers, characterized by a rectangular core, show promise in increasing the achievable expected power limit of circular core fibers. A simple design methodology to determine the core, cladding, and length of an SBS limited fiber amplifier was presented. The design process resulted in a 1.7 m 500x34  $\mu\text{m}$  core ribbon fiber amplifier which could theoretically achieve 10 kW of output power in a single frequency and a single high order mode. This design and simulation of a 10 kW single frequency ribbon fiber laser represents a 5x increase in power above the likely limit for single frequency circular cross-section fibers. Additionally, this 10 kW design is not considered the limit for ribbon fibers, but an example of an amplifier that is not likely to be achieved with a circular cross-section fiber.

Although a manufacturing challenge, the wide dimension could be expanded up to 1 mm, and therefore increase the power above 10 kW, or further shrink the narrow dimension for the same power level. Also, it is clear from Equations (5) and (8) that any increase in the brightness of available diodes would decrease the required length and area to achieve an SBS limited fiber for a particular power level.

The principle of amplifying a single high order mode of a ribbon fiber in a BPM simulation for the purpose of converting to the fundamental mode in free space was demonstrated, and the simulations showed that the purity of the original signal could be maintained even in the absence of any modally selective gain. Although not part of this simulation, modally selective gain has been studied and demonstrated, and could reinforce the single mode status of this proposed amplifier<sup>20</sup>.

This work performed under the auspices of the U.S. Department of Energy by Lawrence Livermore National Laboratory under Contract DE-AC52-07NA27344. (IM release # LLNL-PROC-618439)

## References

- [1] Limpert, J., Roser, F., Klingebiel, S., Schreiber, T., Wirth, C., Peschel, T., Eberhardt, R., and Tiinnermann, A., "The rising power of fiber lasers and amplifiers," *IEEE Journal of Selected Topics in Quantum Electronics* 13(3), 537–545 (2007).

- [2] Dawson, J.W., Messerly, M.J., Beach, R.J., Shverdin, M.Y., Stappaerts, E.A., Sridharan, A.K., Pax, P.H., Heebner, J.E., Siders, C.W., et al., "Analysis of the scalability of diffraction-limited fiber lasers and amplifiers to high average power," *Optics Express* 16(17), 13240 (2008).
- [3] Andrusyak, O., Drachenberg, D., Venus, G.B., Smirnov, V., and Glebov, L.B., "Fiber laser system with kW-level spectrally-combined output," in *Solid State and Diode Laser Technology Review*, 3–7 (2008).
- [4] Drachenberg, D., Divliansky, I., Smirnov, V., Venus, G., and Glebov, L., "High-power spectral beam combining of fiber lasers with ultra high-spectral density by thermal tuning of volume Bragg gratings," in *Proc. of SPIE, Fiber Lasers VII: Technology, Systems, and Applications* 7914(1), J. W. Dawson, Ed., 79141F–1–7914F–10 (2011).
- [5] Jain, A., Drachenberg, D., Andrusyak, O., Venus, G., Smirnov, V., and Glebov, L., "Coherent and spectral beam combining of fiber lasers using volume Bragg gratings," in *Proc. of SPIE, Laser Technology for Defense and Security VI* 7686(1), M. Dubinskii and S. G. Post, Eds., 768615–1–768615–8 (2010).
- [6] Fan, T.Y., "Laser beam combining for high-power, high-radiance sources," *IEEE Journal of Selected Topics in Quantum Electronics* 11(3), 567–577 (2005).
- [7] McNaught, S.J., Asman, Charles, P., Injeyan, H., Jankevics, A., Johnson, A.M., Jones, G.C., Komine, H., Machan, J., Marmo, J., et al., "100-kW coherently combined Nd:YAG MOPA laser array - OSA Technical Digest (CD)," in *Frontiers in Optics, FThD2* (2009).
- [8] Wirth, C., Schmidt, O., Tsybin, I., Schreiber, T., Eberhardt, R., Limpert, J., Tünnermann, A., Ludewigt, K., Gowin, M., et al., "High average power spectral beam combining of four fiber amplifiers to 8.2 kW.," *Optics Letters* 36(16), 3118–20 (2011).
- [9] Ramachandran, S., Fini, J.M., Mermelstein, M., Nicholson, J.W., Ghalimi, S., and Yan, M.F., "Ultra-large effective-area, higher-order mode fibers: a new strategy for high-power lasers," *Laser & Photonics Review* 2(6), 429–448 (2008).
- [10] Cooper, L.J., Wang, P., Williams, R.B., Sahu, J.K., Clarkson, W. a, Scott, a M., and Jones, D., "High-power Yb-doped multicore ribbon fiber laser.," *Optics Letters* 30(21), 2906–8 (2005).
- [11] Khitrov, V., and Shkunov, V., "Er-doped high aspect ratio core (HARC) rectangular fiber producing 5-mJ, 13-nsec pulses at 1572 nm," in *Advanced Solid-State Photonics, AW4A.5* (2012).
- [12] Rockwell, D.A., Shkunov, V. V, and Marciante, J.R., "fiber providing single-mode operation and an ultra-large core area in a compact coilable package," *Optics Express* 19(15), 14746–14762 (2011).
- [13] Rockwell, D., Shkunov, V., and Marciante, J., "Semi-guiding high-aspect-ratio core (SHARC) fiber providing single-mode operation and an ultra-large core area in a compact coilable package," *Optics Express* 19(15), 14746–14762 (2011).
- [14] Beach, R.J., Feit, M.D., Mitchell, S.C., Cutter, K.P., Payne, S.A., Mead, R.W., Hayden, J.S., Krashkevich, D., and Alunni, D. a., "Phase-locked antiguided multiple-core ribbon fiber," *IEEE Photonics Technology Letters* 15(5), 670–672 (2003).
- [15] Bullington, A.L., Pax, P.H., Sridharan, A.K., Heebner, J.E., Messerly, M.J., and Dawson, J.W., "Mode conversion in rectangular-core optical fibers.," *Applied Optics* 51(1), 84–8 (2012).

- [16] Sridharan, A., Pax, P.H., Heebner, J.E., Drachenberg, D.R., Armstrong, P.J., and Dawson, J.W., "Mode-converters for rectangular-core fiber amplifiers to achieve diffraction-limited power scaling," *Optics Express* 20(27), 28792–28800 (2012).
- [17] Smith, R., "Optical power handling capacity of low loss optical fibers as determined by stimulated Raman and Brillouin scattering," *Applied Optics* 11(11), 2489–2494 (1972).
- [18] Giles, C.R., and Desurvire, E., "Modeling erbium-doped fiber amplifiers," *Journal of Lightwave Technology* 9(2), 271–283 (1991).
- [19] Gapontsev, V., and Gapontsev, D., "2 kW CW ytterbium fiber laser with record diffraction-limited brightness," in *Lasers and Electro-optics Europe* 12(25), 508 (2005).
- [20] Beach, R.J., Feit, M.D., Page, R.H., Brasure, L.D., Wilcox, R., and Payne, S. a., "Scalable antiguided ribbon laser," *Journal of the Optical Society of America B* 19(7), 1521 (2002).
- [21] Yeh, P., and Yariv, A., "Bragg reflection waveguides," *Optics Communications* 19(3), 427–430 (1976).
- [22] SeGall, M., Rotar, V., Lumeau, J., Mokhov, S., Zeldovich, B., and Glebov, L.B., "Binary volume phase masks in photo-thermo-refractive glass.," *Optics letters* 37(7), 1190–2 (2012).
- [23] Mohammed, W., Pitchumani, M., Mehta, A., and Johnson, E., "Selective excitation of the LP<sub>11</sub> mode in step index fiber using a phase mask," *Optical Engineering* 45(7), 074602 (2006).
- [24] Fienup, J.R., "Phase retrieval algorithms: a comparison.," *Applied Optics* 21(15), 2758–69 (1982).